^{182}Hf–^{182}W age dating of a ^{26}Al-poor inclusion and implications for the origin of short-lived radioisotopes in the early Solar System

Jesper C. Holst[a], Mia B. Olsen[a], Chad Paton[a], Kazuhide Nagashima[b], Martin Schiller[a], Daniel Wielandt[a], Kirsten K. Larsen[a], James N. Connelly[a], Jes K. Jørgensen[c], Alexander N. Krot[a,b], Åke Nordlund[c], and Martin Bizzarro[a,1]

[a]Centre for Star and Planet Formation and Natural History Museum of Denmark, University of Copenhagen, DK-1350 Copenhagen, Denmark; [b]Hawaii Institute of Geophysics and Planetology, University of Hawaii at Manoa, Honolulu, HI 96822; and [c]Centre for Star and Planet Formation and Niels Bohr Institute, University of Copenhagen, DK-2100 Copenhagen, Denmark

Edited by Neta A. Bahcall, Princeton University, Princeton, NJ, and approved April 18, 2013 (received for review January 8, 2013)

Refractory inclusions [calcium–aluminum-rich inclusions, (CAIs)] represent the oldest Solar System solids and provide information regarding the formation of the Sun and its protoplanetary disk. CAIs contain evidence of now extinct short-lived radioisotopes (e.g., ^{26}Al, ^{41}Ca, and ^{182}Hf) synthesized in one or multiple stars and added to the protosolar molecular cloud before or during its collapse. Understanding how and when short-lived radioisotopes were added to the Solar System is necessary to assess their validity as chronometers and constrain the birthplace of the Sun. Whereas most CAIs formed with the canonical abundance of ^{26}Al corresponding to $^{26}Al/^{27}Al$ of $\sim 5 \times 10^{-5}$, rare CAIs with fractionation and unidentified nuclear isotope effects (FUN CAIs) record nucleosynthetic isotopic heterogeneity and $^{26}Al/^{27}Al$ of $< 5 \times 10^{-6}$, possibly reflecting their formation before canonical CAIs. Thus, FUN CAIs may provide a unique window into the earliest Solar System, including the origin of short-lived radioisotopes. However, their chronology is unknown. Using the ^{182}Hf–^{182}W chronometer, we show that a FUN CAI recording a condensation origin from a solar gas formed coevally with canonical CAIs, but with $^{26}Al/^{27}Al$ of $\sim 3 \times 10^{-6}$. The decoupling between ^{182}Hf and ^{26}Al requires distinct stellar origins: steady-state galactic stellar nucleosynthesis for ^{182}Hf and late-stage contamination of the protosolar molecular cloud by a massive star(s) for ^{26}Al. Admixing of stellar-derived ^{26}Al to the protoplanetary disk occurred during the epoch of CAI formation and, therefore, the ^{26}Al–^{26}Mg systematics of CAIs cannot be used to define their formation interval. In contrast, our results support ^{182}Hf homogeneity and chronological significance of the ^{182}Hf–^{182}W clock.

meteorite inclusions | short-lived radionuclides | Solar System formation

Meteorites and their components contain evidence for the presence of now extinct short-lived ($t_{1/2} < 10$ Ma) radionuclides (e.g., ^{41}Ca, ^{26}Al, ^{60}Fe, ^{53}Mn, and ^{182}Hf) during the earliest stages of the Solar System's evolution. These radioisotopes are believed to have an external, stellar origin, and were either inherited from the ambient interstellar medium or injected into the protosolar molecular cloud before or contemporaneously with its collapse (1). Understanding how and when these radioisotopes were added to the nascent Solar System can constrain the astrophysical environment where our Sun formed and, therefore, test models of Solar System formation. The oldest Solar System solids preserved in chondritic meteorites are calcium–aluminum-rich inclusions (CAIs), which define an absolute age of 4,567.30 ± 0.16 Ma (2). These millimeter-to-centimeter objects are believed to have formed as fine-grained condensates from a ^{16}O-rich gas of approximately solar composition in a region with high ambient temperature (>1,300 K) and low total pressures ($\sim 10^{-4}$ bar). This environment existed in the innermost part of the protoplanetary disk during the early stage of its evolution characterized by high mass accretion rates ($\sim 10^{-5}\ M_\odot\ y^{-1}$) to the proto-Sun (3). Formation of CAIs near the proto-Sun is also indicated by the presence in these objects of the short-lived radioisotope ^{10}Be formed by solar energetic particle irradiation (4). Some of the CAIs subsequently experienced melting and evaporation to form distinct coarser igneous inclusions, such as the compact Type A and Type B CAIs commonly observed in CV meteorites (carbonaceous chondrite of the Vigarano type) (5).

The majority of CAIs in unmetamorphosed chondrites contain high abundance of radiogenic ^{26}Mg (^{26}Mg*), the decay product of ^{26}Al ($t_{1/2} \sim 0.7$ Ma), corresponding to an inferred initial $^{26}Al/^{27}Al$ ratio of $\sim(4.5–5.5) \times 10^{-5}$ (6). Recent high-precision ^{26}Al–^{26}Mg systematics of bulk CV CAIs define the so-called canonical $^{26}Al/^{27}Al$ ratio of $(5.252 \pm 0.019) \times 10^{-5}$ (7). The uncertainty of the canonical $^{26}Al/^{27}Al$ ratio corresponds to ~4,000 y, implying a brief episode of condensation and melt evaporation that resulted in Al/Mg fractionation event(s). However, it is uncertain whether the canonical $^{26}Al/^{27}Al$ ratio reflects that of the bulk Solar System or, alternatively, only a local snapshot of the evolving inhomogeneous protoplanetary disk.

A rare subset of refractory grains [platy hibonite crystals (PLACs) and blue aggregates (BAGs), ref. 8] and inclusions (6, 9) have low initial $^{26}Al/^{27}Al$ ratios ($< 5 \times 10^{-6}$). Of particular interest are the coarse-grained igneous inclusions with fractionation and unidentified nuclear effects (FUN CAIs, ref. 10), which, in addition to their low initial abundance of ^{26}Al, are characterized by large mass-dependent fractionation effects and nucleosynthetic anomalies in several elements. These observations are interpreted to reflect formation of FUN CAIs by thermal processing of presolar dust aggregates before the injection of ^{26}Al and its homogenization in the protoplanetary disk (11). If this interpretation is correct, FUN CAIs can provide insights into the timing of admixing of ^{26}Al to the forming protoplanetary disk and, in turn, the origin of short-lived radioisotopes in the early Solar System. However, a late formation of ^{26}Al-poor CAIs after decay of ^{26}Al cannot be excluded. Indeed, CAIs are known to have experienced multistage thermal processing in the protoplanetary disk and/or on their chondrite parent bodies (5) that could have erased their radiogenic ^{26}Mg. Thus, obtaining a robust age estimate for a FUN inclusion is a critical step toward a better understanding of the significance of ^{26}Al-poor inclusions.

Author contributions: J.C.H. and M.B. designed research; J.C.H., M.B.O., C.P., K.N., M.S., D.W., K.K.L., J.N.C., and M.B. performed research; J.C.H., M.B.O., C.P., K.N., M.S., D.W., J.N.C., J.K.J., A.N.K., Å.N., and M.B. analyzed data; and J.C.H., A.N.K., and M.B. wrote the paper.

The authors declare no conflict of interest.

This article is a PNAS Direct Submission.

Freely available online through the PNAS open access option.

[1]To whom correspondence should be addressed. E-mail: bizzarro@snm.ku.dk.

This article contains supporting information online at www.pnas.org/lookup/suppl/doi:10.1073/pnas.1300383110/-/DCSupplemental.

Results and Discussion

Most known FUN CAIs were discovered >30 y ago and were largely consumed during destructive isotopic measurements. To identify additional FUN CAIs suitable for age dating, we conducted a systematic search of coarse-grained refractory inclusions in the Allende CV carbonaceous chondrite, given that CV chondrites contain the highest proportion of igneous CAIs among the distinct chondrite groups. Of ∼220 inclusions investigated, only one FUN CAI was identified on the basis of its bulk magnesium–isotope composition. This FUN inclusion, named STP-1, is a coarse-grained igneous Type B2 CAI composed of melilite, spinel, Al,Ti-diopside, and anorthite. STP-1 contains only minor amounts of secondary minerals (nepheline, sodalite, grossular, and monticellite), indicating that it largely avoided secondary alteration processes. Similar to most previously identified FUN CAIs (10, 12), STP-1 shows mass-dependent enrichment in the heaviest isotopes of magnesium, as well as deficits in the mass-independent components of ^{26}Mg (^{26}Mg*) and ^{54}Cr of ∼300 and ∼3,500 ppm, respectively (Table 1). Trace element analysis demonstrates that STP-1 is characterized by a Group II rare-earth element (REE) pattern (Fig. 1), indicative of condensation from a gas depleted in the most refractory REEs (13). On a three-isotope oxygen diagram, compositions of spinel, anorthite, hibonite, and most Al,Ti-diopside grains plot along a mass-dependent fractionation line with a slope of 0.52 and Δ^{17}O value of –24 ± 1‰. Oxygen–isotope compositions of melilite and some Al,Ti-diopside grains deviate from this line and show Δ^{17}O values ranging from −17 to –4‰ and from –24 to –17‰, respectively (Fig. 2). The igneous texture and the fractionated magnesium and oxygen–isotope composition favoring the heaviest isotopes imply that STP-1 experienced melt evaporation at low total pressure (14) following condensation of its precursor material. To define the initial abundance of ^{26}Al at the time of crystallization of STP-1, we have investigated the ^{26}Al–^{26}Mg systematics of its primary minerals by secondary ionization mass spectrometry. Multiple analyses of spinel, Al,Ti-diopside, melilite, hibonite, and anorthite crystals define an internal isochron corresponding to an initial ^{26}Al/^{27}Al ratio of (2.94 ± 0.21) × 10^{-6} (Fig. 3*A*), that is, much lower than the canonical value of ∼5 × 10^{-5}.

Absolute age dating of CAIs by the Pb–Pb method requires knowledge of the uranium–isotope composition of individual inclusions (2). However, the uranium concentration in STP-1 is depleted by a factor of ∼100 compared with canonical CAIs, possibly due to loss during melt evaporation under oxidizing conditions. As such, STP-1 in particular, and FUN inclusions in general, may not be suited for uranium-corrected absolute Pb–Pb dating using current state-of-the-art mass spectrometry techniques. To define the formation age of STP-1, we have instead investigated its ^{182}Hf–^{182}W systematics by the internal isochron approach. With a half-life of ∼9 Ma, the ^{182}Hf-to-^{182}W decay scheme is one of the most widely used chronometers to understand the timing of solid formation in the early Solar System (15). In addition, currently available data support the proposal that the ^{182}Hf nuclide was uniformly distributed in the early Solar System with an initial ^{182}Hf/^{180}Hf ratio of (9.85 ± 0.40) × 10^{-5} (16–18). First, the ^{182}Hf–^{182}W isochron of canonical CAIs intersects the carbonaceous chondritic composition, suggesting that the precursor material of primitive asteroids that presumably accreted in the outer Solar System had similar initial ^{182}Hf content as CAIs (16). Second, there is excellent agreement between uranium-corrected Pb–Pb and Hf–W ages of rapidly cooled magmatic meteorites (19). Lastly, CAIs with variable tungsten nucleosynthetic anomalies define the same initial ^{182}Hf abundance (17), indicating that the source of ^{182}Hf is decoupled from that responsible for nucleosynthetic heterogeneity in refractory elements such as tungsten. The Al,Ti-diopside, anorthite and melilite fractions separated from STP-1 define a statistically significant ^{182}Hf–^{182}W isochron corresponding to an initial ^{182}Hf/^{180}Hf ratio of (9.60 ± 1.10) × 10^{-5} and intercept of –113 ± 27 ppm, when the ^{186}W/^{183}W is used to correct for instrumental mass fractionation (Fig. 3*B*). Using a different isotope pair for internal normalization yields an identical initial ^{182}Hf/^{180}Hf within uncertainty but a different intercept of –26 ± 26 ppm (see the legend of Fig. 3). These two intercept values are distinct from the inferred Solar System initial μ^{182}W value of – 351 ± 10 ppm (18), indicating the presence of tungsten nucleosynthetic heterogeneity in STP-1. In contrast, the internal ^{182}Hf–^{182}W isochron of STP-1 corresponds to a ^{182}Hf/^{180}Hf ratio that is identical within analytical uncertainty to the Solar System initial ^{182}Hf/^{180}Hf ratio of (9.85 ± 0.40) × 10^{-5} inferred from canonical CAIs (18). Accepting the inferred initial ^{182}Hf/^{180}Hf ratio of STP-1 and associated uncertainty at face value, we calculate an age difference of $0.33^{-1.47}_{+1.67}$ Ma between formation of STP-1 and canonical CAIs, which is not consistent with the time interval of $3.02^{-0.07}_{+0.08}$ Ma inferred from the ^{26}Al–^{26}Mg system. Thus, we conclude that the formation age of STP-1 and, by extension, that of ^{26}Al-poor FUN CAIs, is coeval with canonical CAIs within the uncertainty of our measurements. These results are consistent with the proposal that ^{182}Hf was homogeneously distributed in the solar protoplanetary disk at the time of formation of the Solar System's first solids (16–18).

The contrasting initial abundances of ^{26}Al recorded by CAIs with identical initial ^{182}Hf/^{180}Hf ratios indicate that ^{26}Al was heterogeneously distributed in the protoplanetary disk during the epoch of CAI formation. Therefore, the ^{26}Al–^{26}Mg systematics of CAIs cannot be used to define the duration of the CAI-forming event(s). Likewise, the apparently restricted range of inferred initial ^{26}Al/^{27}Al ratios defined by bulk analyses of canonical CAIs from CV carbonaceous chondrites does not necessarily imply a homogeneous distribution of ^{26}Al throughout the solar protoplanetary disk during and after the epoch of CAI formation. Assessing the degree of ^{26}Al homogeneity in the disk requires careful comparison between the ^{26}Al–^{26}Mg and uranium-corrected Pb–Pb ages of objects with simple thermal histories. We note that the age difference between the formation of canonical CAIs and rapidly cooled angrite meteorites inferred from the assumption-free uranium-corrected Pb–Pb dating method is not consistent with that suggested by the ^{26}Al–^{26}Mg system,

Table 1. ^{182}Hf–^{182}W systematics of mineral fractions and bulk Mg and Cr isotope compositions of the STP-1 FUN CAI

Sample	^{27}Al/^{24}Mg	μ^{25}Mg	μ^{26}Mg*	μ^{53}Cr	μ^{54}Cr	^{180}Hf/^{183}W	$\mu^{182}W_{(6/3)}$	$\mu^{184}W_{(6/3)}$	$\mu^{182}W_{(6/4)}$	$\mu^{183}W_{(6/4)}$
Bulk	3.18 ± 0.06	9,331 ± 20	−303 ± 10	260 ± 9	−3,579 ± 15					
Melilite						1.978 ± 0.119	−18 ± 27	−28 ± 15	69 ± 22	41 ± 23
Anorthite						2.675 ± 0.161	35 ± 27	−27 ± 16	115 ± 35	43 ± 24
Diopside						14.22 ± 0.85	622 ± 52	−31 ± 24	676 ± 58	46 ± 37

Isotope ratios expressed in the μ-notation, which reflect 10^6 (ppm) deviations from the terrestrial reference standard. Uncertainties represent the external reproducibility or internal precision, whichever is larger. Mg and Cr isotope data were acquired following techniques outlined in Bizzarro et al. (33) and Trinquier et al. (34), respectively. (6/3), internally normalized to ^{186}W/^{183}W; (6/4), internally normalized to ^{186}W/^{184}W.

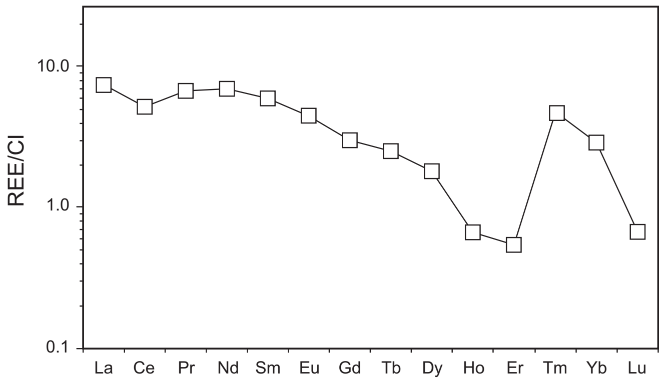

Fig. 1. Chondrite-normalized bulk REE abundances in the Allende STP-1 FUN CAI. This CAI is characterized by a Group II REE pattern and a small negative Ce anomaly.

supporting widespread ^{26}Al heterogeneity in the solar protoplanetary disk (2, 7).

The decoupling between the initial abundances of ^{26}Al and ^{182}Hf in early-formed refractory inclusions requires distinct stellar sources to account for the presence of these short-lived nuclides in the early Solar System. In addition, the Hf–W data reported here for the STP-1 FUN CAI are most easily understood in the context of a homogeneous distribution of ^{182}Hf at the birth of the Solar System. If correct, this implies that the carrier of this short-lived radioisotope was well mixed within the Solar System's parental molecular cloud. Heavy *r*-process isotopes such as ^{182}Hf are thought to be synthesized during the explosions of core-collapse supernovae of less than 11 $M_\odot$ (20). Because the lifetime of these "lower mass" massive stars is significantly longer than the typical lifetime of giant molecular clouds (21), they are not expected to contribute appreciable amounts of freshly synthesized radionuclides into star-forming regions. Therefore, in agreement with models of the chemical evolution of the galaxy (20, 22), we infer that the initial ^{182}Hf/^{180}Hf ratio of ~1×10^{-4} recorded by FUN and canonical CAIs reflects long-term, steady-state galactic stellar nucleosynthesis before the formation of the protosolar molecular cloud. A galactic origin for ^{182}Hf in the early Solar System is consistent with the view that this radionuclide was homogeneously distributed in the protoplanetary disk at the time of formation of the Solar System's first solids as inferred from earlier work and the ^{182}Hf–^{182}W data presented here for the STP-1 FUN inclusion.

In contrast with ^{182}Hf, the Solar System's initial inventory of ^{26}Al is approximately 10 times higher than the background levels of the galaxy inferred from γ-ray astronomy (23) and/or models of the galactic chemical evolution (20, 22), requiring late-stage addition of stellar debris to the Solar System's parental molecular cloud. A possibility is that the observed variable ^{26}Al abundances during the epoch of CAI formation reflect heterogeneity in the CAI precursor material (24). Such heterogeneity could result from selective thermal processing of presolar carriers, including the carrier(s) of ^{26}Al, thereby generating reservoirs enriched or depleted in presolar components (25). However, ^{26}Al-poor objects such as FUN CAIs, PLACs, and BAGs show large-scale nucleosynthetic heterogeneity in the stable ^{48}Ca and ^{50}Ti nuclides, including both enrichments and depletions (8, 10, 12, 26, 27), implying that the heterogeneity preserved in these objects is unrelated to ^{26}Al. Moreover, the mineralogy of STP-1, coupled with its group II REE pattern and ^{16}O-rich composition, suggest that the precursor material of this inclusion formed by condensation from a gas of solar composition depleted in the most refractory REEs, similar to the majority of fine-grained CAIs. Thus, although it is possible that the variable nucleosynthetic anomalies present in ^{26}Al-poor objects reflect selective thermal processing of their precursors, we conclude that the initial ^{26}Al/^{27}Al of ~3×10^{-6} recorded by STP-1 represents the ^{26}Al abundance in the CAI-forming region when this inclusion crystallized.

Solids ultimately thermally processed in the CAI-forming region are believed to represent molecular cloud material accreting to the proto-Sun from the infalling envelope via the protoplanetary disk (28). In contrast with ^{182}Hf, our results suggest that the carrier of ^{26}Al was heterogeneously distributed in the protosolar molecular cloud and, by extension, during infall of envelope material to the protoplanetary disk. However, at the time of formation of the earliest Solar System solids, the innermost protoplanetary disk is thought to have been physically well mixed (29), implying that the observed ^{26}Al heterogeneity during formation of FUN and canonical CAIs may be temporal rather than spatial. Thus, the different levels of ^{26}Al in these inclusions could reflect admixing of stellar derived carrier(s) of ^{26}Al to the protoplanetary disk during the epoch of CAI formation. Progressive admixing of ^{26}Al to the disk can be understood in the framework of the inside-out collapse model of prestellar cores, where the innermost portion of the core collapses first, followed by the successive outer layers (30). This interpretation requires the innermost part of the protostellar molecular cloud to have been depleted in ^{26}Al compared with the remaining cloud, and that the formation of FUN CAIs predates canonical CAIs, the latter being allowed by the ^{182}Hf–^{182}W age uncertainty of the STP-1 FUN CAI.

A galactic origin for the initial abundance of ^{182}Hf recorded by the FUN and canonical CAIs requires ~18 Ma of free decay between last nucleosynthetic event that produced the heavy

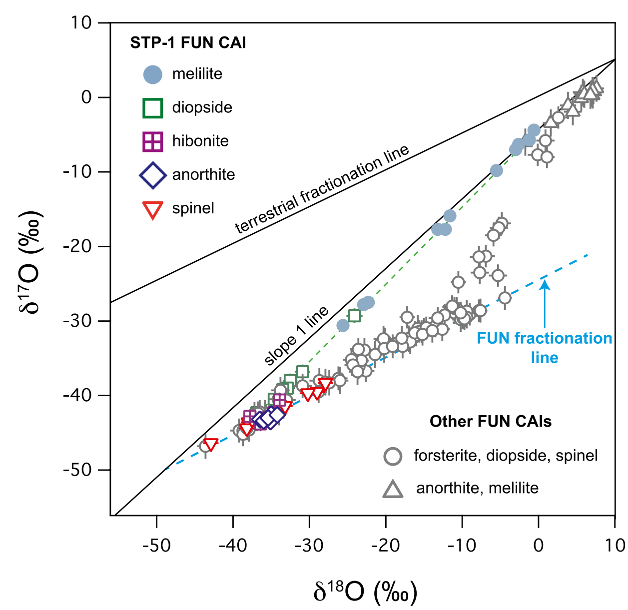

Fig. 2. Three-isotope oxygen diagram of oxygen–isotope compositions of individual minerals in the Allende STP-1 FUN CAI. Similarly to the majority of FUN CAIs (31), the oxygen–isotope compositions of anorthite, spinel, hibonite, and most Al,Ti-diopside grains in STP-1 plot along a mass-dependent fractionation line defining an initial Δ^{17}O value of ~ −24‰, that is, similar to the oxygen–isotope composition of canonical CAIs and that of the Sun (31, 32). Oxygen–isotope compositions of melilite and some of the Al,Ti-diopside grains plot along a line with a slope of ~1, suggesting subsequent isotope exchange with a ^{16}O-depleted gaseous reservoir. In contrast with most FUN CAIs from CV chondrites characterized by ^{16}O-poor compositions of melilite and anorthite, melilite in STP-1 shows a range of Δ^{17}O values, whereas anorthite is uniformly ^{16}O-rich. These observations indicate that STP-1 is more pristine than all previously known FUN CAIs.

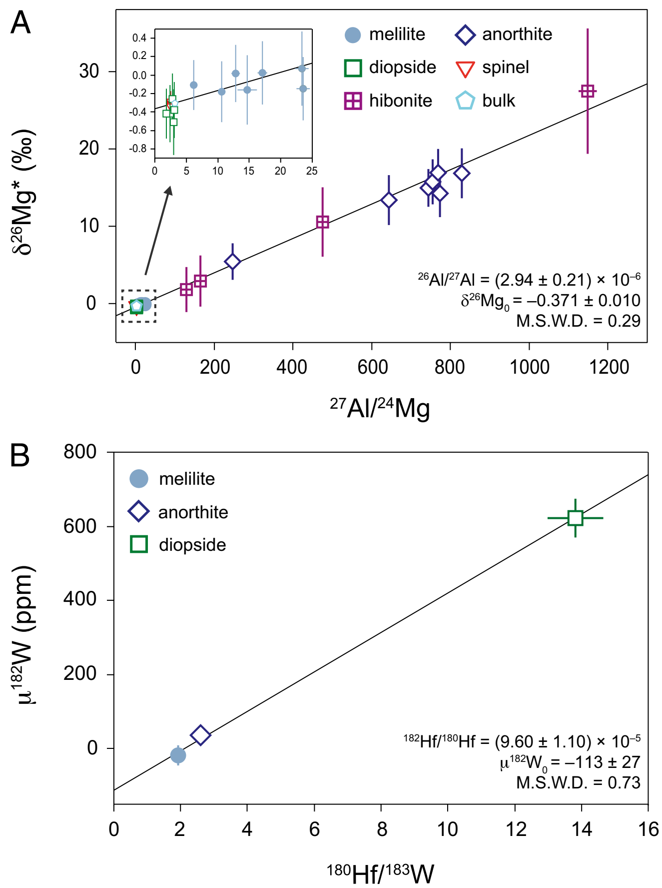

Fig. 3. Internal mineral ^{26}Al–^{26}Mg (*A*) and ^{182}Hf–^{182}W (*B*) isochron diagrams for the Allende STP-1 FUN CAI. The well-defined ^{26}Al–^{26}Mg isochron based on spinel, Al,Ti-diopside, melilite, anorthite, and hibonite shows no evidence for late-stage disturbance, consistent with its pristine mineralogy and the ^{16}O-rich composition of most primary phases. Thus, we infer that the ^{26}Al–^{26}Mg isochron defines the initial $^{26}Al/^{27}Al$ ratio in STP-1 at the time of its crystallization. M.S.W.D., mean square of weighted deviations. Using the $^{186}W/^{184}W$ instead of the $^{186}W/^{183}W$ ratio for internal normalization returns an initial $^{182}Hf/^{180}Hf$ value of $(9.22 \pm 1.1) \times 10^{-5}$ and an intercept of -26 ± 26 ppm (M.S.W.D. = 0.31). This $^{182}Hf/^{180}Hf$ value is identical within analytical uncertainty to that obtained using the $^{186}W/^{183}W$ for internal normalization, although marginally lower. However, repeated analysis of a number of distinct aliquots of column-processed BCR-2 (Basalt, Columbia River) rock standard and the Allende carbonaceous chondrite using a quantity of W comparable to that present in the mineral fractions of the STP-1 FUN CAI indicates a superior external reproducibility when the $^{186}W/^{183}W$ is used for internal normalization. Therefore, our preferred approach is to use the $^{186}W/^{183}W$ for internal normalization, in agreement with earlier studies (17, 18, 35, 36).

r-process nuclides and formation of the Solar System (22). This time interval, however, is not compatible with the initial $^{26}Al/^{27}Al$ ratio of $\sim 3 \times 10^{-6}$ defined by the STP-1 FUN CAI, accepting that this value represents that of the ^{26}Al-poor region of the protosolar molecular cloud before the last addition of freshly synthesized ^{26}Al present in canonical CAIs. If correct, this interpretation suggests that the protosolar molecular cloud was part of a giant molecular cloud complex (GMC) chemically enriched in freshly synthesized matter by earlier generation(s) of massive stars to account for the level of ^{26}Al present in FUN CAIs. Whether our Sun formed during the early or late evolutionary stages of the GMC requires knowledge of the $^{60}Fe/^{26}Al$ value of canonical and FUN CAIs, given that most of the ^{26}Al in the early life of the GMC will be synthesized and ejected by the stellar winds of massive stars where ^{60}Fe is not produced.

Materials and Methods

We conducted a systematic search for new FUN CAIs by investigating the Mg–isotope composition of numerous igneous CAI-like objects in cut sections of an ~3 kg fragment of the Allende CV carbonaceous chondrite. All igneous CAI-like inclusions of appropriate size were sampled with a computer-assisted microdrilling device fitted with 300-μm–diameter diamond-coated microdrills. The sampled material was digested using hydrofluoric (HF)–HNO_3 acid mixtures and, after complete dissolution, a 5% aliquot of the sample was taken for Al/Mg ratio determination to 5% accuracy using a ThermoFisher X-Series II inductively coupled plasma source mass spectrometer (ICPMS) at the Centre for Star and Planet Formation in Copenhagen. The magnesium from samples with Al/Mg ratios typical of CAIs was purified by ion-exchange chromatography and its isotopic composition analyzed using a ThermoFisher Neptune multiple collector inductively coupled plasma source mass spectrometer (MC-ICPMS) at the Centre for Star and Planet Formation in Copenhagen, following protocols outlined in Bizzarro et al. (33). One inclusion was typified by a resolvable deficit in $^{26}Mg^*$ of ~300 ppm as well as a stable Mg–isotope composition enriched in the heavy isotopes by ~1%/amu. This inclusion, named STP-1, was classified as a FUN CAI and selected for further analysis. Present on the surfaces of two 3-mm–thick sections, the STP-1 FUN CAI is a spherical inclusion of ~10 mm in diameter. Once the inclusion was liberated from the Allende meteorite, polished sections were made from the extracted material for petrographic characterization, mineral chemistry and in situ ^{26}Al–^{26}Mg and O–isotope work.

Elemental maps of sections and electron microprobe analyses of individual minerals were performed with the University of Hawaii (UH) field-emission electron JEOL JXA-8500F operated at 15-kV accelerating voltage, 15-nA beam current, and fully focused beam using five wavelength spectrometers. The STP-1 inclusion is a coarse-grained igneous CAI composed of pure anorthite, gehlenitic melilite ($Åk_{6-28}$), and igneously zoned Al,Ti-diopside (Al_2O_3 = 17.7 −28.5 wt %, TiO_2 = 0.03–8.7 wt %), all poikilitically enclosing euhedral compositionally pure spinel grains. Lath-shaped hibonite grains and spinel–hibonite intergrowths occur in the outermost portion of the inclusion. The hibonite grains have low contents of MgO (0.2–1.7 wt %) and TiO_2 (0.09–3.2 wt %). No multilayered Wark–Lovering rim sequence is observed around STP-1. The oxygen isotope composition and Al–Mg systematics of primary minerals in STP-1 was investigated using the UH Cameca ims-1280 ion microprobe based on techniques described in *SI Materials and Methods*.

Following removal from the Allende slab and cleaning, bulk fragments of STP-1 were preserved for bulk isotope and elemental analyses. The remaining material was gently crushed in an agate mortar under distilled ethanol and minerals were handpicked under binocular microscopes in both plain and back lighting. REE abundances were determined on the X-Series II ICPMS from a bulk aliquot of STP-1, using sample-standard bracketing techniques. The chromium isotope composition of a separate bulk aliquot was determined based on previously published techniques (34) using a ThermoFisher Triton thermal ionization mass spectrometer at the Centre for Star and Planet Formation. Following handpicking, the anorthite, melilite, and Al,Ti-diopside fractions were rinsed in distilled ethanol followed by 0.02 M HNO_3 in an ultrasonic bath for 15 min. After complete dissolution in mixtures of concentrated $HF:HNO_3:H_2O_2$, a 15% aliquot of each sample was extracted and spiked with a mixed $^{180}Hf/^{186}W$ tracer for elemental abundance determinations. Tungsten was purified by ion-exchange chromatography in a two-step procedure inspired from Fritz et al. (37) and Strelow et al. (38). Samples were dissolved in 0.25 M HNO_3 + 0.1 M HF + 0.1% H_2O_2 and loaded on a column containing 2–4 mL of AG50W-X8 resin, and W was eluted along with high-field strength elements with 1–2 column volumes (c.v.) of 0.25 M HNO_3 + 0.1 M HF + 0.1% H_2O_2 followed by 2.5 c.v. of 0.1 M HF. After dry down, samples were dissolved in 1 M HF and loaded on a column containing 1 mL AG1-X4 resin. Residual elements were eluted sequentially with 5 c.v. of 1 M HF, 5 c.v. of 2 M HCl + 0.1% H_2O_2 and 2 c.v. of 6 M HCl + 0.01 M HF, whereas the W was recovered with 4 c.v. of 6 M HCl + 1 M HF.

Following tungsten purification, isotope data were acquired in static mode using the ThermoFisher Neptune MC-ICPMS at the Centre for Star and Planet Formation. Samples were converted to nitrate form, dissolved in a 2% HNO_3 solution containing traces of HF, and introduced into the plasma source by means of an Aridus II desolvating nebulizer. Mass fractionation was corrected with the exponential law using the $^{186}W/^{183}W$ = 1.98594 (39). Samples were analyzed only once, and the ratios are reported as relative deviations from the mass-bias corrected NIST 3163 tungsten reference material in the μ-notation (10^6 deviations). A blank correction was applied to all samples, and the uncertainty of this correction is propagated in the final uncertainties of the isotope measurements reported in Table 1. Full analytical details of procedures used for Hf/W and W isotope measurements, as well as all other data reported in this paper, are presented in *SI Materials and Methods*.

ACKNOWLEDGMENTS. We thank G. J. Wasserburg for comments on an earlier version of this paper. We also thank Andy Davis and two anonymous referees for their constructive comments, which improved the quality of this paper. The Centre for Star and Planet Formation is financed by the Danish National Research Foundation (Grant DNRF97).

1. Goswami JN (2004) Short-lived radionuclides in the early solar system: The stellar connection. *New Astron Rev* 48:125–132.
2. Connelly JN, et al. (2012) The absolute chronology and thermal processing of solids in the solar protoplanetary disk. *Science* 338(6107):651–655.
3. D'Alessio P, Calvet N, Woolum DH (2005) *Chondrites and the Protoplanetary Disk*, eds Krot AN, Scott ERD, Reipurth B (Astrophysical Society of the Pacific, San Francisco), Vol 341, pp 353–372.
4. McKeegan KD, Chaussidon M, Robert F (2000) Incorporation of short-lived ^{10}Be in a calcium-aluminum-rich inclusion from the allende meteorite. *Science* 289(5483): 1334–1337.
5. MacPherson GJ (2003) *Treatise on Geochemistry 1*, ed Davis AM (Elsevier, Amsterdam), pp 201–246.
6. Krot AN, et al. (2009) Origin and chronology of chondritic components: A review. *Geochim Cosmochim Acta* 73:4963–4997.
7. Larsen KK, et al. (2011) Evidence for magnesium isotope heterogeneity in the solar protoplanetary disk. *Astrophys J* 735:L37.
8. Liu M-C, et al. (2009) Isotopic records in CM hibonites: Implications of timescales for mixing of isotope reservoirs in the solar nebula. *Geochim Cosmochim Acta* 73:5051–5079.
9. Makide K, et al. (2011) Heterogeneous distribution of ^{26}Al at the birth of the solar system. *Astrophys J* 733:L31.
10. Wasserburg GJ, Lee T, Papanastassiou DA (1977) Correlated O and Mg isotopic anomalies in Allende inclusions: II. Magnesium. *Geophys Res Lett* 4:299–302.
11. Sahijpal S, Goswami JN (1998) Refractory phases in primitive meteorites devoid of ^{26}Al and ^{41}Ca: Representative samples of first solar system solids? *Astrophys J* 509:L137–L140.
12. Papanastassiou DA, Brigham CA (1989) The identification of meteorite inclusions with isotope anomalies. *Astrophys J* 338:L37–L40.
13. Boynton WV (1975) Fractionation in the solar nebula: Condensation of yttrium and the rare earth elements. *Geochim Cosmochim Acta* 39:569–584.
14. Richter FM, Janney PE, Mendybaev RA, Davis AM, Wadhwa M (2007) Elemental and isotopic fractionation of Type B CAI-like liquids by evaporation. *Geochim Cosmochim Acta* 71:5544–5564.
15. Kleine T, et al. (2009) Hf-W chronology of the accretion and early evolution of asteroids and terrestrial planets. *Geochim Cosmochim Acta* 73:5150–5188.
16. Kleine T, Mezger K, Palme H, Scherer E, Münker C (2005) Early core formation in asteroids and late accretion of chondrite parent bodies: Evidence from ^{182}Hf-^{182}W in CAIs, metal-rich chondrites and iron meteorites. *Geochim Cosmochim Acta* 69: 5805–5818.
17. Burkhardt C, et al. (2008) Hf-W mineral isochron for Ca,Al-rich inclusions: Age of the solar system and the timing of core formation in planetesimals. *Geochim Cosmochim Acta* 72:6177–6197.
18. Burkhardt C, Kleine T, Dauphas N, Wieler R (2012) Nucleosynthetic tungsten isotope anomalies in acid leachates of the Murchison meteorite: Implication for hafnium-tungsten chronometry. *Astrophys J* 753:L6.
19. Kleine T, Hans U, Irving AJ, Bourdon B (2012) Chronology of the angrite parent body and implications for core formation in protoplanets. *Geochim Cosmochim Acta* 84:186–203.
20. Huss GR, Meyer BS, Srinivasan G, Goswami JN, Sahijpal S (2009) Stellar sources of the short-lived radionuclides in the early solar system. *Geochim Cosmochim Acta* 73: 4922–4945.
21. Murray N (2011) Star formation efficiencies and lifetimes of giant molecular clouds in the Milky Way. *Astrophys J* 729:133.
22. Wasserburg GJ, Busso M, Gallino R, Nollett KM (2006) Short-lived nuclei in the early solar system: Possible AGB sources. *Nucl Phys A* 777:5–69.
23. Diehl R, et al. (2006) Radioactive ^{26}Al from massive stars in the Galaxy. *Nature* 439 (7072):45–47.
24. Wood JA (1998) Meteoritic evidence for the infall of large interstellar dust aggregates during formation of the solar system. *Astrophys J* 503:L101–L104.
25. Trinquier A, et al. (2009) Origin of nucleosynthetic isotope heterogeneity in the solar protoplanetary disk. *Science* 324(5925):374–376.
26. Fahey A, Goswami JN, McKeegan KD, Zinner E (1985) Extreme ^{50}Ti enrichments in primitive meteorites. *Astrophys J* 196:L17–L20.
27. Ireland T (1990) Presolar isotopic and chemical signatures in hibonite-bearing refractory inclusions from the Murchison carbonaceous chondrite. *Geochim Cosmochim Acta* 54:3219–3237.
28. Williams JP, Cieza LA (2011) Protoplanetary disks and their evolution. *Annu Rev Astron Astrophys* 49:67–117.
29. Boss AP (2011) Evolution of the solar nebula. IX. Gradients in the spatial heterogeneity of the short-lived radioisotopes ^{60}Fe and ^{26}Al and the stable oxygen isotopes. *Astrophys J* 739:61.
30. Myers PC, Evans NJ II, Ohashi N (2000) in *Protostars and Planets IV*, eds Boss AP, Russell SS (Univ of Arizona Press, Tucson), pp 217–245.
31. Krot AN, et al. (2010) Oxygen isotopic composition of the sun and mean oxygen isotopic composition of the protosolar silicate dust: Evidence from refractory inclusions. *Astrophys J* 713:1159–1166.
32. McKeegan KD, et al. (2011) The oxygen isotopic composition of the Sun inferred from captured solar wind. *Science* 332(6037):1528–1532.
33. Bizzarro M, et al. (2011) High-precision Mg-isotope measurements of terrestrial and extraterrestrial material by HR-MC-ICPMS – implications for the relative and absolute Mg-isotope composition of the bulk silicate earth. *J Anal At Spectrom* 26:565–577.
34. Trinquier A, Birck J-L, Allègre CJ (2008) High-precision analysis of chromium isotopes in terrestrial and meteorite samples by thermal ionization mass spectrometry. *J Anal At Spectrom* 23:1565–1574.
35. Scherstén A, Elliott T, Hawkesworth C, Norman M (2004) Tungsten isotope evidence that mantle plumes contain no contribution from the Earth's core. *Nature* 427(6971): 234–237.
36. Schérsten A, Elliott T, Hawkesworth C, Russell S, Masarik J (2006) Hf-W evidence for rapid differentiation of iron meteorites parent bodies. *Earth Planet Sci Lett* 241: 530–542.
37. Fritz JS, Garralda BB, Karraker SK (1961) Cation exchange separation of metal ions by elution with hydrofluoric acid. *Anal Chem* 33:882–886.
38. Strelow FWE, Weinert CHSW, Eloff C (1972) Distribution coefficients and anion exchange behavior of elements in oxalic acid–hydrochloric acid mixtures. *Anal Chem* 44: 2352–2356.
39. Völkening J, Köppe M, Heumann KG (1991) Tungsten isotope ratio determinations by negative thermal ionization mass spectrometry. *Int J Mass Spectrom Ion Process* 107: 361–368.